ASSESSMENT OF GROUND CONDITIONS NEAR A MINE PORTAL USING GROUND PENETRATING RADAR

Michael A. Trevits, Research Physical Scientist
William D. Monaghan, Electrical Engineer
NIOSH - Pittsburgh Research Laboratory
Pittsburgh, PA

Thomas P. Mucho, President,
Thomas P. Mucho & Associates, Inc.
Washington, PA

ABSTRACT

The NIOSH Lake Lynn Laboratory (LLL) is a unique research facility, located about 50 miles southeast of Pittsburgh, Pennsylvania, that is designed to provide a full-scale mining environment for testing and evaluation of mine health and safety technologies. The LLL occupies more than 400 acres and is composed of surface test and training areas and an underground mine. The Lake Lynn Experimental Mine (LLEM) was built at an abandoned commercial limestone quarry where surface mining ceased in the late 1960's. Later, new underground development was constructed to simulate modern-day coal mining scenarios; including room-and-pillar and longwall mining layouts. In January 1994, a sinkhole opened southeast of the No. 4 Portal of the LLEM and since then, the area of the underground failure and surface deformation has continued to expand and now includes several interconnected sinkholes. A concern developed that the overburden instability could expand and affect the structural integrity of the nearby highwall and the No. 4 Portal. It was unsafe to conduct a detailed underground survey of the mine in this area because the mine roof conditions near the No. 4 Portal had deteriorated significantly. It was decided to investigate the overburden conditions near the No. 4 Portal using ground penetrating radar (GPR). A GPR survey grid was located along an access road that passes over the top of the portal. To delineate the mine conditions near the portal, antennas whose frequency spectra produced pulses centered near 100- and 200-MHz were used. The results of the GPR survey suggests that the overburden rock units appear to be laterally consistent to a depth of about 15-ft. Below that point, the overburden appears to be significantly disturbed and it was hypothesized that this area contains a large roof fall. A follow-up ground truth survey of the mine roof conditions was conducted from the mouth of the portal. It is concluded that the observations and measurements made from the radar records appear to be correct as a large roof fall was observed and measured from the mine portal area.

INTRODUCTION

The NIOSH Lake Lynn Laboratory (LLL) is a unique research facility, located about 50 miles southeast of Pittsburgh, Pennsylvania. LLL is designed to provide a full-scale mining environment for the testing and evaluation of mine health and safety technologies. LLL occupies more than 400 acres and is composed of surface test and training areas and an underground mine (Lake Lynn Experimental Mine (LLEM)) (figure 1). From a geological perspective, the mine has been developed in the Mississipian Age Greenbriar Limestone unit of the Mauch Chunk Formation and is locally known as the Wymps Gap Limestone (formally known as the "Greenbriar of Pennsylvania"). The units exposed are typically gray, hard, and massive with a few interbedded shale units (1).

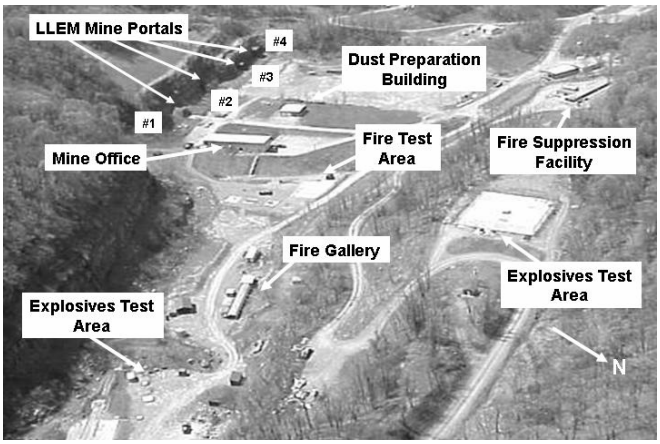

Figure 1. Lake Lynn Laboratory

The LLEM was built at an abandoned commercial limestone quarry (figure 2). The mine workings on the west side of the property are known as the "old workings" with entries 49-ft wide by 33-ft high. These workings were developed by a commercial limestone aggregate operation when surface mining ceased in the late 1960's. Later, under the direction of the U.S. Bureau of Mines, 7,545 ft of new underground development was constructed on the east side of the property using 19.7-ft wide by 6.6-ft high entries (this area is known as the "new workings"). The new workings have been configured to simulate modern-day coal mining scenarios; including room-and-pillar and longwall mining layouts (2, 3). Roof support in the primary escapeway areas of the mine is provided through the use of fully-grouted roof bolts and screens. During development of the new workings, fully-grouted roof bolts were installed.

In late January 1994, a large roof fall occurred in the old workings near the Nos. 3 and 4 Portals and in close proximity to the highwall (figure 3). Since the area of the fall occurred near the outcrop, the overburden was relatively shallow (about 100 ft) and the upward growth of the roof fall broke through to the surface forming a sinkhole (4). With time, the area of the underground failure and surface deformation has continued to expand and now includes an area of several interconnected sinkholes (figure 4).

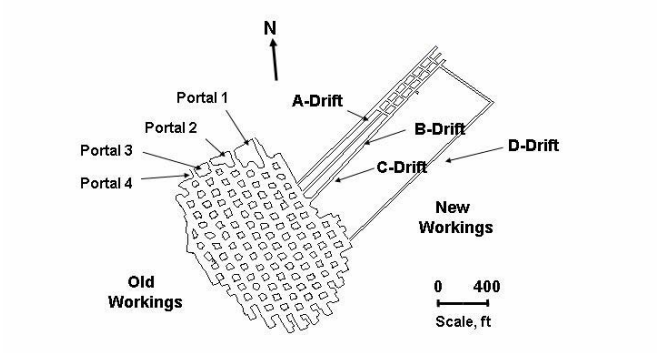

Figure 2. Lake Lynn Experimental Mine

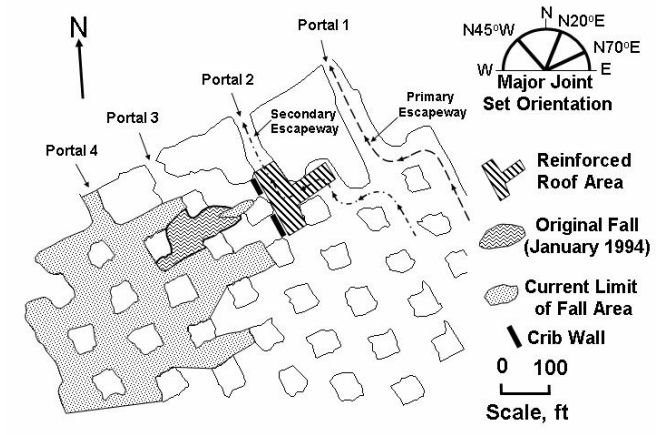

Figure 3. Map of roof fall area in the old workings.

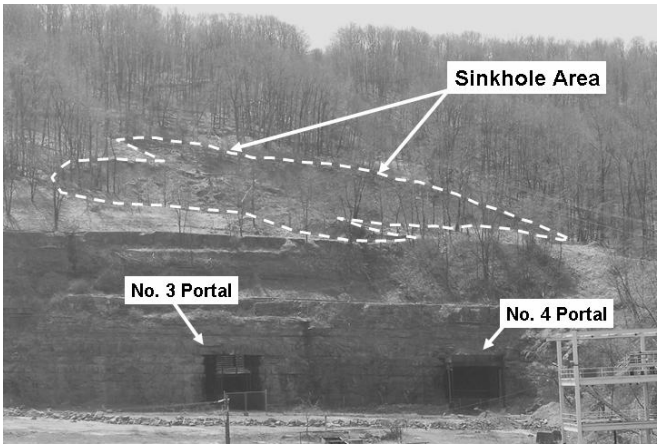

Figure 4. View of mine portal Nos. 3 and 4 and sinkhole area.

The conditions leading up to the roof collapse have been studied in detail from a geologic and engineering perspective and several factors have been identified that most likely contributed to the roof collapse. These factors are summarized as follows from the literature (4-6). As mentioned earlier, the Greenbriar Limestone at this site contains several interbedded limestone and shale units. Rock mass ratings of the roof material using two different systems (Norwegian Geotechnical Institute and Bieniawski's Rock Mass Rating systems) showed the mine roof at the LLEM to be in the "good" range with recommended permanent width openings no greater than 50 ft and between 90 and 150 ft for temporary openings (4). Although the mine entry spans in the old workings are about 50 ft, intersection spans approach 75 ft. In addition, the staggered pillar design employed in the old workings also resulted in significant roof spans (5). It is interesting to note that the mine roof failure in January 1994 did indeed occur in an intersection.

At the mine site, there are three nearly vertical sets of joints sets. A prominent joint set trends nearly parallel to the highwall at N70^{o}E and two less significant joint sets are oriented at N20^{o}E and N45^{o}W (figures 3 and 5). In some areas of the old workings, water can be observed dripping intermittently from the exposed joints especially during periods of precipitation. In the area of the collapse, the joints outlined large blocks of limestone in the mine roof. It is believed that over time, water percolated through and eroded the joint sets, followed by an infilling of sandy clay material (thereby reducing the overall rock mass strength) (4, 5).

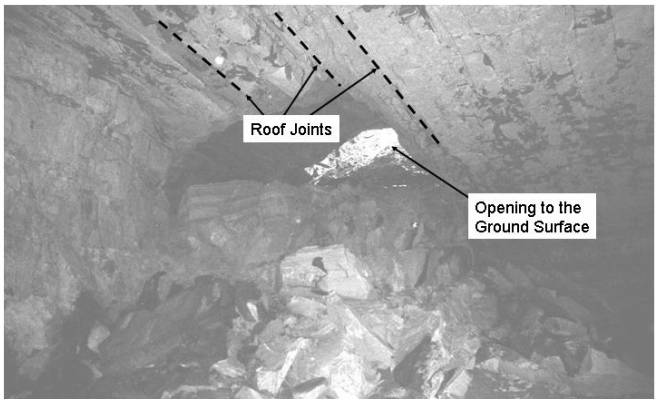

Figure 5. View of mine roof near sinkhole.

Finally, weather conditions may have been the triggering mechanism leading to the mine roof collapse. The cold winter weather at LLL typically causes significant ice build-up along the highwall and in the portal areas. During the month of January 1994, temperatures were extremely cold followed by a sudden warming trend that allowed snow to melt on the surface above the mine thus increasing the amount of water in the overburden. The highwall ice barriers could have restricted water flow from the overburden thus causing a build-up of water pressure and thereby reducing the stress applied normal to the joints. The reduction in normal stress reduced the frictional resistance along joint surfaces. This process could have also caused the joint-outlined roof rock to slide along the joint planes to a level that allowed the roof to collapse (4).

There was a concern that the roof failure could expand in two directions to include the secondary escapeway of the LLEM. It was decided to reinforce and protect the secondary escapeway and to install instrumentation to monitor the changing conditions in the

mine roof (figure 6). This work is described in detail by Dolinar (4). There was additional concern that the overburden instability could also expand and affect the structural integrity of the highwall and the No. 4 Portal. To monitor conditions along the highwall areas, several survey monuments were installed along the edge of the highwall and surveys of the position of the monuments are collected monthly. In addition, four biaxial tiltmeters were also installed along select areas of the surface deformation (figure 7). These instruments are connected to a datalogger that collects ground movement on an hourly basis. Over time, the mine roof conditions near the No. 4 Portal had deteriorated significantly and it was too dangerous to conduct a detailed underground survey of the mine in this area. It was therefore decided to investigate the overburden conditions near the No. 4 Portal remotely using GPR.

Figure 6. Crib wall to protect the secondary escapeway.

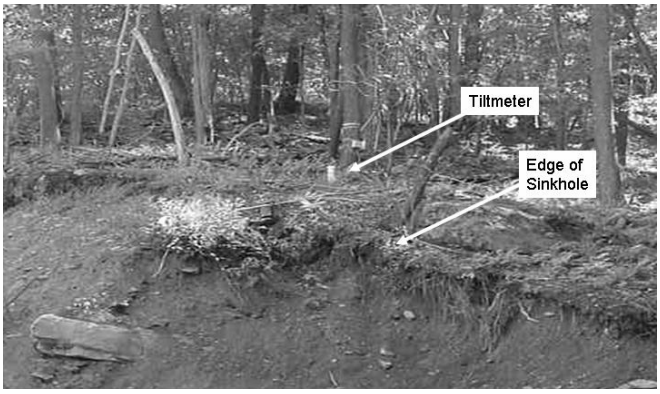

Figure 7. Biaxial tiltmeter installed at edge of sinkhole.

GROUND PENETRATING RADAR TECHNOLOGY

GPR has been used in agricultural, archeological, construction, environmental, forensic, geological, groundwater, military, and mining applications (7)[1]. Under the proper conditions, GPR can provide valuable information that can be integrated into the mining plans to help define problematic areas or identify the problem sources. Advance identification of the areas can allow mine operators to plan for changing ground conditions or avoid predicted problem areas (8). Use of dynamic GPR surveys (surveys performed while moving the antenna at a constant pace) can generate large quantities of field data and, under certain circumstances, can provide detailed subsurface information of a scope that is superior to that obtained from single-point sources such as drill holes (note, the collection of ground truth information to verify the radar interpretations is always recommended). Because of greater sample density, anomalous zones are more likely to be detected by GPR as compared to drilling, resulting in a more accurate characterization of subsurface conditions (9).

GPR is a non-invasive geophysical method that uses reflected and backscattered electromagnetic waves to locate and identify variations in the electrical properties of subsurface materials (7). The basic principles of reflective ground penetrating radar are summarized as follows (10). An electromagnetic pulse wave is radiated into the ground from a transmitting antenna and travels at a velocity that is primarily determined by the relative permittivity of the material. The wave radiates outward until it encounters material with different electrical properties. At that point, a portion of the energy passes through the material, some of the energy is refracted away and part of the energy is reflected back to the source. The reflected portion of the wave is captured by a receiving antenna and is recorded for processing. The round trip time (or two-way travel time) of the pulse is greater for deeply buried material or objects than for shallow material or objects. Therefore, the time of arrival for the reflected wave can be used to determine the approximate depth to a feature (fracture, void, geological structure, etc), if the velocity of the wave in the subsurface is known.

There are two important electrical properties of geological materials that affect the pulse wave – dielectric constant (relative permittivity) and conductivity. Dielectric constant is a critical parameter because it controls the propagation velocity of electromagnetic waves through a material and the reflection coefficients at interfaces, as well as affecting the vertical and horizontal imaging resolution (11). In rocks and minerals, dielectric properties are primarily a function of mineralogy, porosity, water saturation, frequency, lithology, component geometries, and electrochemical interactions (11-13). Variations in each of these parameters can significantly change bulk dielectric constants (11). The value of the dielectric constant ranges from 1 for air (fastest propagation) to 81 for water (slowest propagation) and the greater the difference between the two materials, the stronger the reflected pulse wave (14). Table 1 shows select reported values for dielectric constants.

Table 1. Reported values of select bulk dielectric constants.

Rock Type, Condition	Bulk Dielectric Constant
Coal, dry	3.5 (15)
Coal, wet	8 (15)
Limestone, dry	5.5 (14)
Limestone, wet	8 (15)
Sandstone, dry	2-3 (15)
Sandstone, wet	5-10 (15)
Shale (Condition Not Reported)	5-15 (15)
Shale, wet	6-9 (15)

[1] Additional information on GPR can be found on the Internet using search terms such as “ground penetrating radar”, “GPR”, “georadar”, “ground probing radar”, “subsurface radar”, “borehole radar”, borehole GPR”, etc (www.g-p-r.com is a good starting point) .

Electrical conductivity is the ability of a material to conduct electrical current, and it determines the depth of penetration of the pulse wave, i.e., greater conductivity results in lesser depth of penetration. Conductivity can vary greatly and is primary governed by water content and dissolved salts, as well as the density, permeability, porosity, and the temperature of the material (16).

Antenna selection for mining applications will be dictated by the size, orientation and depth of the feature under investigation and the ability to securely hold or move the antenna along the mine roof, rib areas or along the ground surface. If sufficiently sized samples of the host rock can be obtained or if in-mine calibration tests can be performed, then it is possible to accurately estimate the dielectric constant of the material and thus make reliable estimates of the depth and location of the in-situ material, object or feature under study. In general, a contrast in properties has to occur over a size larger than 1/3 of a wavelength to be observable (though 1/10 wavelength is possible under exceptional circumstances) (7). Radar survey resolution increases with increasing antenna frequency (decreasing wavelength), but at the expense of depth of investigation (which generally improves with decreasing antenna frequency) (7). In other words, high-frequency antennas can provide high resolution, but have shallow depths of penetration and lower-frequency antennas have lower resolution and deeper depths of penetration (17). For further information about antenna wavelength and resolution, an in-depth discussion is provided in reference 7.

OBJECTIVE and APPROACH

The objective of this work was to determine if GPR could be used to help assess the mine roof conditions near the No. 4 Portal area of the Lake Lynn Experimental Mine (LLEM). The GPR surveys were conducted using shielded antennas whose frequency spectra produced pulses centered near 100-MHz (set in the bistatic position) and 200-MHz (figure 8). These antennas were selected because they were expected to provide the required depth of penetration (the 30 ft thickness of the overburden) with the necessary resolution (ability to resolve the mine opening or roof fall area) and could be easily moved along an old access road that served as the survey site over the No. 4 Portal.

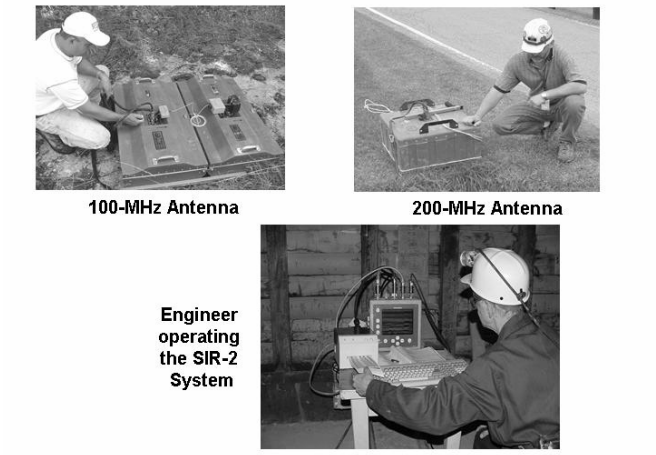

Figure 8. SIR 2 System and antennas used in this study.

The equipment used to conduct the ground penetrating radar survey in this study was a GSSI SIR® System 2 (SIR-2) Model No. DC-2 control unit (figure 8) built by Geophysical Survey Systems, Inc.[2] The SIR-2 is a lightweight, portable, general-purpose radar system that is available as an intrinsically safe unit. The output display can be shown as a single wiggle trace (a waveform display plot that is analogous to an oscilloscope trace), a waterfall plot of the wiggle traces (shows multiple stacked radar waveforms), or a multicolored line scan (reflected signal amplitudes represented by various colors according to a user-selected color look-up table). The data can also be printed via an external printer.

RADAR SURVEY

A GPR survey grid was located along an access road that passed over the top of portal No. 4 (figure 9). In the area of the access road, the soil and unconsolidated weathered rock units had been removed exposing the limestone rock mass, thus allowing for good coupling of the transmitted radar wave with the rock units. Three survey lines were positioned on the access road and reference stations were placed on each line about 10 ft apart (labeled A-I). Survey line L1 (survey stations 1A-1I) and L2 (survey stations 2A-2I) were each 80 ft long and trended approximately perpendicular to the portal. Survey line L3 (survey stations 3B-3G) was positioned parallel to L2 and was only 60 ft in length due to a nearby hillside that limited surface access (figure 10). A tape measurement showed that the overburden at the No. 4 Portal was 30 ft thick. A layout map of the survey grid is shown in figure 11.

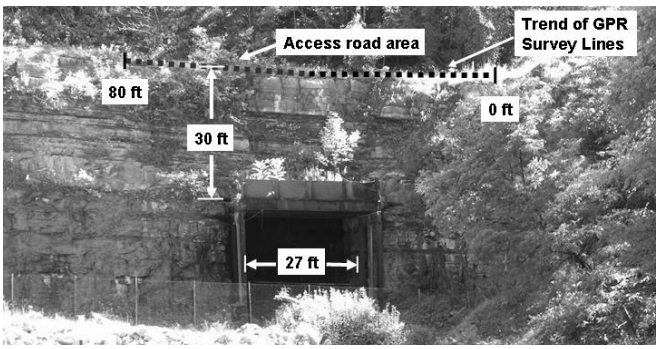

Figure 9. LLEM Portal No. 4. Note relative position of GPR survey line is shown as the black dotted line.

Dynamic scans of the area were made over the grid following the trend of each survey line. Reference marks were placed at 10 ft intervals along each line in the radar record to mark the start and end of the line, and at the edge of the No. 4 Portal. Table 2 shows the SIR-2 system set-up for each antenna used in this study. The values shown in the table, with the exception of the vertical high- and low-pass filter settings, scans per second and the dielectric constant, are standard default values. Adjustments to the vertical low-pass filter settings were made to eliminate high-frequency noise (snow) from the data. Adjustments to vertical high-pass filter settings were made to eliminate low-frequency noise (tilt) from the data (14). A dielectric constant of 6.0 was used in this study based on results from previous radar work at the LLEM; these studies included calibration experiments (18). Although several interbedded zones of shale were observed in the outcrop, it was believed that the value of the dielectric constant used was

[2] Mention of a specific product or trade name does not imply endorsement by NIOSH.

reasonable for this study site since the most prominent rock units appeared in the correct location in the processed radar records when compared to highwall measurements.

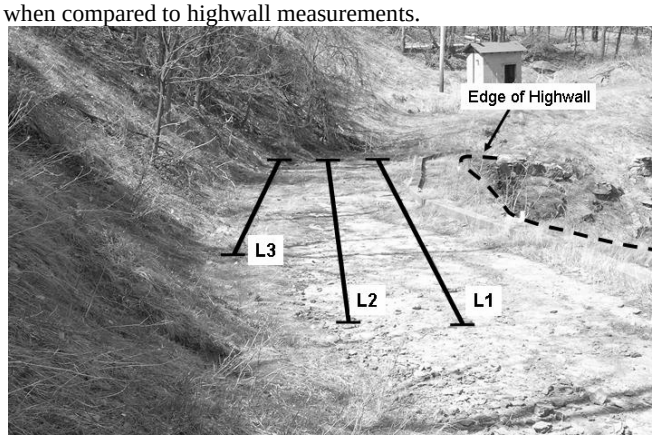

Figure 10. Layout of the GPR survey area near Portal No. 4.

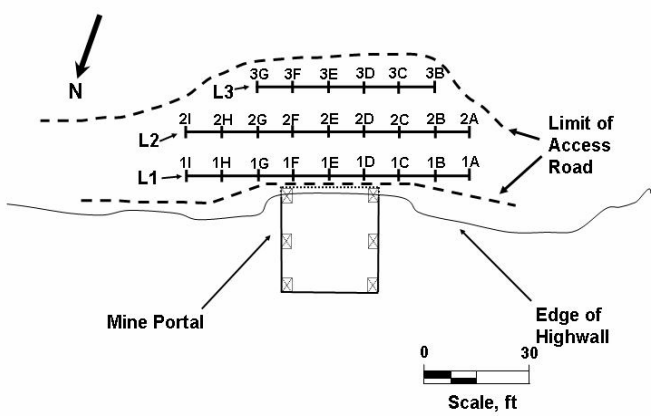

Figure 11. Map of the GPR survey area near Portal No. 4.

Table 2. SIR 2 set-up used for GPR survey.

Parameter	100-MHz Antenna	200-MHz Antenna
Data collection mode	Continuous	Continuous
Range, ns	300-600	200
Samples per scan	2048	1024
Resolution, bits	16	16
Number of gain points	4	5
Vertical high pass filter, MHz	15	30
Vertical low pass filter, MHz	200	400
Scans per second	16	32
Horizontal Smoothing, scans	5	5
Transmit Rate, KHz	32	64
Dielectric Constant	6 (18)	6 (18)

RADAR RECORD INTERPRETATION

The radar records generated during this study were analyzed using GSSI's Radar Data Analyzer for Windows (RADAN)[3] version 6.0. This package allows the user to operate in the Windows environment with application-specific modules (19). Figures 12-14 show examples of interpreted radar records from surveys of each line using the 200-MHz antenna to a depth of about 20 ft. The vertical scale in all figures represents depth into the limestone and the horizontal scale represents distance along the survey line. Short vertical line segments were added to the horizontal scale showing the beginning and end of the survey, reference survey points, and the edges of the portal. In all of the radar records, the reflected pulse energy is shown in terms of a grayscale, with near-white being the highest level of reflected pulse energy and near-black the lowest. Areas in the record shown with similar gray tones should be interpreted as similar levels of reflected pulse energy. In figure 12, a disturbed or failed zone is believed to extend across the No. 4 Portal opening to a depth of about 10-ft below the ground surface (as outlined by the dotted ellipse). In figure 13, a fractured or disturbed zone is believed to extend near the middle to the left edge of the No. 4 portal opening at a depth of about 10-ft below the ground surface. It is possible that the high energy reflector (shown as near-white in the figure) observed at about 9 ft deep is a zone that may contain water (perhaps a zone containing shale). The loss of this signal return in the middle area of the image may be due to loss of water through the joints or fractures in the disturbed zone. These same reflections are seen in figure 12 with a similar lateral disruption of the reflected energy wave over the disturbed roof zone. In figure 14, it appears that there are two shallow zones, extending to a depth of 5- to 10-ft below the ground surface (outlined by dotted ellipses), that show a disruption in the lateral continuity of the reflected energy wave. These zones may represent fractured or jointed areas. Below that, extending from the middle to the right edge of the No. 4 Portal (outlined by the dotted ellipse), is another zone of disrupted energy wave reflections. Again, it is thought that this area may represent a fractured or disturbed zone.

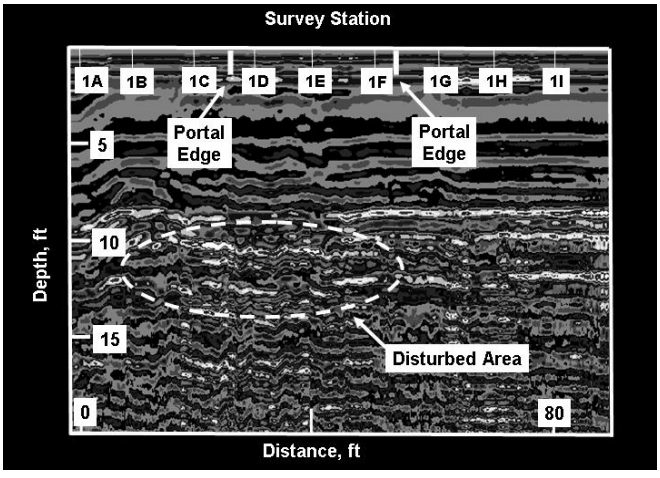

Figure 12. Interpreted radar record for Line 1 (200-MHz antenna).

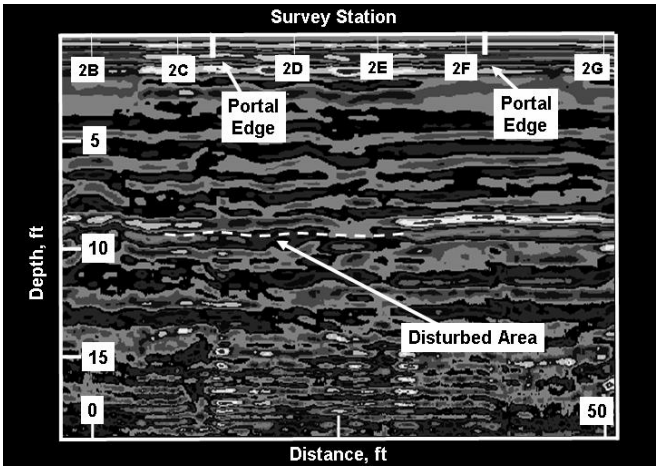

Figure 13. Interpreted radar record for Line 2 (200-MHz antenna).

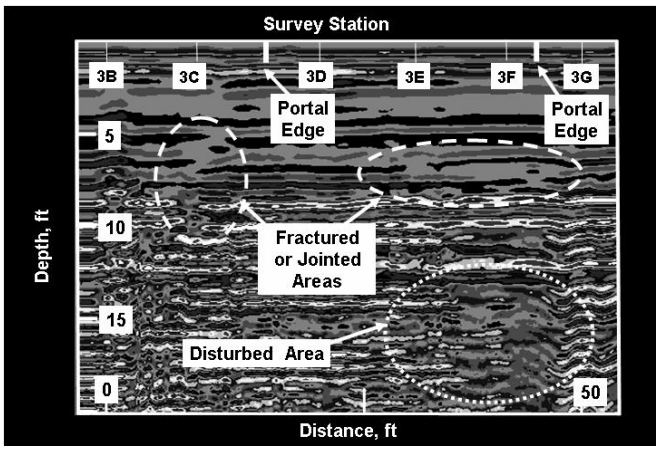

Figure 14. Interpreted radar record for Line 3 (200-MHz antenna).

Figures 15 and 16 show examples of interpreted radar records from surveys of L1 and L2 respectively using the 100-MHz antenna. Note, a lower depth of penetration is shown in the record than those presented for the 200-MHz antenna (refer to the previous discussion on antenna resolution and depth of penetration). In figure 15, a downward trending disturbed zone extends from survey reference point 1A through to survey reference point 1H. The beginning of the disturbed zone appears to start at a depth of 15 ft near survey reference point 1A and then gradually progresses downward to a depth of about 20 ft near survey reference point 1H. In the record, two high-energy reflections (areas shown as near-white in the figure) are also seen, one leading upward from the bottom of the figure towards reference point 1C and the other, though less prominent, leading upwards towards reference point 1F. These reflections are most likely the supports for the metal structure positioned at the opening of the portal (refer to figure 9). In figure 16, the overburden rock units appear to be laterally consistent to a depth of about 12 to 15 ft. Below that point, from survey reference point 2B extending to the right edge of Portal No. 4, the overburden appears to be significantly disturbed. In the record, high-energy reflections (again areas shown as near-white in the figure) are also seen at the bottom of the figure below survey reference points 2D, 2E and 2F. These reflections are again most likely the supports for the metal structure positioned at the opening of the portal (refer to figure 9). The fact that the energy reflections shown in figure 16 are not as prominent as those shown in figure 15 is most likely because L2 is positioned farther away from the metal structure than L1. It is believed that the disturbed area of the mine roof shown in figures 15 and 16 extends one-half the thickness of the overburden above the portal, about 15-ft, or downward to the first instance of disruption at a depth of 15-ft.

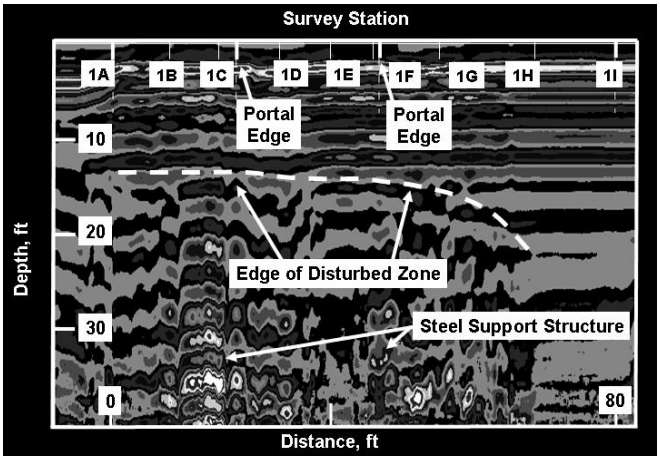

Figure 15. Interpreted radar record for Line 1 (100-MHz antenna).

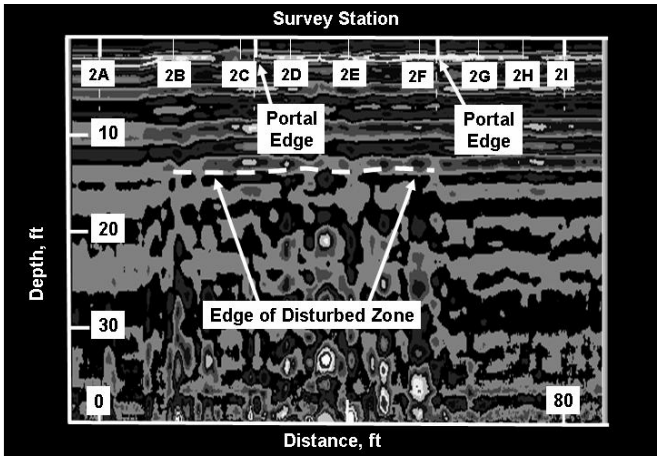

Figure 16. Interpreted radar record for Line 2 (100-MHz antenna).

GROUND TRUTH SURVEY

A follow-up ground truth survey of the mine roof conditions was conducted remotely from a safe area at the mouth of the portal. The observations made from the radar records appear to be correct as a large roof fall was observed near the mouth of the portal (figure 17). A close-up view of the roof conditions near the mouth of Portal No. 4 is shown in figure 18. In this figure, the roof fall appears to extend to right and towards the A to C survey reference points (note in the radar records the disturbed zones also generally extended through these survey points). Laser distance measurements of the height of the mine roof, made from the mouth of the portal show the collapsed area was within about 15 ft of the ground surface. These measurements are also in general agreement with the observations made from the 100- and 200-MHz radar records.

Figure 17. View of conditions near the opening of Portal No. 4.

Figure 18. Close-up view of roof conditions near the opening of Portal No. 4.

SUMMARY and CONCLUSIONS

In late January 1994, a large roof fall occurred in the old workings of the LLEM and extended upward to the ground surface forming a large sinkhole. Over time, the roof fall area and the surface disturbance continued to grow. There was concern that the roof fall area could extend and negatively affect the secondary escapeway of the LLEM and highwall area. Supplemental mine roof support was installed underground along with monitoring stations to chart the movement of the mine roof, highwall and ground surface near the sinkhole areas. Because of limited underground access due to extensive roof falls, it was decided to survey the conditions of the mine roof near the No. 4 Portal using GPR. Three survey lines were located on an access road that extended over the No. 4 Portal. GPR surveys were performed using 100- and 200-MHz antennas. The results of the surveys suggest that the effects of the mine roof disturbance extend to within 10- to 15-ft of the ground surface. A follow-up ground truth survey of the No. 4 Portal area, though limited in lateral extent, seems to confirm the observations made from the radar records. It is concluded from this study that GPR surveys using 100- and 200-MHz antennas can provide detailed information about the upward extent of mine roof falls in areas of shallow overburden thickness and locations where surface soils and unconsolidated weathered rock units are not a factor.

ACKNOWLEDGMENTS

The authors would like to recognize the valuable help and knowledgeable assistance of the following individuals during the review of this paper: Dr. Syd S. Peng, Chairman and C.T. Holland Professor, West Virginia University; Dr. Gary L. Mowery, Mining Engineer, NIOSH, George Gardner, Mining Engineer, MSHA; and Thomas A. Gray, Engineering Manager II, GAI Consultants, Inc.

REFERENCES

1. Shultz, C.H., The Geology of Pennsylvania, Pennsylvania Geological Survey Special Publication 1, 1999, p. 143-144.

2. National Institute for Occupational Safety and Health, Lake Lynn Laboratory (flyer), Pittsburgh, PA: U.S. Department of Health and Human Services, Public Health Service, Centers for Disease Control and Prevention, National Institute for Occupational Safety and Health, DHHS (NIOSH) Publication No. 99-149, 1999, 1 p.

3. Triebsch, G.F. and M.J. Sapko, Lake Lynn Laboratory: A State-of-the-Art Mining Research Laboratory, in Proceedings of the International Symposium on Unique Underground Structures, June 12-15, 1990, Denver, CO, Chapter 75, pp. 75-1 to 75-21.

4. Zelanko, J.C., T.P. Mucho, A. T. Iannacchione, T. M. Barczak, Stabilization of a Large Shallow, Potentially Unstable Underground Opening, Proceedings of the 2nd North American Rock Mechanics Symposium: NARMS'96, Montreal, Quebec, Canada, June 19-21, 1996, pp. 155-161.

5. Dolinar, D.R., T.E. Marshall, T.M., Barczak, and T.P. Mucho, Stability of Underground Openings Adjacent to the Sinkhole at the NIOSH Lake Lynn Laboratory, SME Annual Meeting Preprint No. 03-154, Cincinnati, OH, February 24-26, 2003, 7 p.

6. Iannacchione, A.T., Mucho, T.P. and L. J. Prosser, Ground Control Problems in the Underground Limestone Industry, Proceedings of the Environment, Safety and Health Forum (National Stone Association), Nashville, TN, October 22-24, 1995, 24 pp.

7. Olhoeft, G.R., Home Page, Introduction and History of Ground Penetrating Radar, http://www.g-p-r.com/introduc.htm, November 15, 2004 (indicates date visited).

8. Trevits, M.A., W.D. Monaghan, and T.P. Mucho, Use of Ground Penetrating Radar Technology for Mining Applications, SME Annual Meeting Preprint No. 05-129, Salt Lake City, UT, February 28-March 2, 2005, 13 p.

9. Technos, Surface Geophysical Methods – An Improved Approach, Volume 1, Issue 1, Fall 2004, 20 p.

10. Daniels, J.J., Ground Penetrating Radar Fundamentals, Prepared as an Appendix to a report to the US EPA, Region V, Department of Geological Sciences, The Ohio State University, November 25, 2000, 21 p.

11. Martinez, A, and Byrnes, A.P., Modeling Dielectric-Constant Values of Geologic Materials: An Aid to Ground-Penetrating Radar Data Collection and Interpretation, Current Research in Earth Sciences, Bulletin 247, Part 1, 2001, 16 p.

12. Knight, R, and A. Endres, A New Concept in Modeling the Dielectric Response of Sandstones: Defining a Wetted Rock and Bulk Water System; Geophysics 55, No. 5, 1990, pp. 586-594.

13. Knoll, M.D., A Petrophysical Basis for Ground-Penetrating Radar and Very Early Time Electromagnetics, Electrical Properties of Sand-Clay Mixtures, Ph.D. dissertation, University of British Columbia, 1996, 316 p.

14. Geophysical Survey Systems, Inc., SIR System 2 Operation Manual, Revision A – May 1996, 101 p.

15. Daniels, D. J., Surface-Penetrating Radar—IEE Radar, Sonar, Navigation and Avionics Series 6: London, The Institute of Electrical Engineers, 1996, 320 p.

16. Mowrey, G.L., C.W. Ganoe, and W.D. Monaghan, A Radar-Based Highwall Rib-Thickness Monitoring System. Proceedings of the SME 1995 Annual Meeting, SME Pre-Print No. 95-163, Denver, CO, March 6-9, 1995, 5 p.

17. GeoModel, Ground Penetrating Radar, Basic Operating Principles, http://www.geomodel.com/gprtext.htm, November 15, 2004 (indicates date visited).

18. Monaghan, W.D., M.A. Trevits, T.P. Mucho and J. Wood, Recent National Institute for Occupational Safety and Health Research Using Ground Penetrating Radar for Detection of Mine Voids. Proceedings of the Geophysical Techniques for Detecting Underground Coal Mine Voids – An Interactive Forum, Lexington, Kentucky, July 29-30, 2003, 29 p.

19. Geophysical Survey Systems, Inc., RADAN 6 Users Manual, MN43-171, 2004, 135 p.